KAPL-P-000009
(K95082)

CONF-9507247--

RECEIVED
AUG 20 1998
OSTI

CHARACTERISTICS OF INDIUM OXIDE PLASMA FILTERS DEPOSITED BY ATMOSPHERIC PRESSURE CHEMICAL VAPOR DEPOSITION

E. Brown, R. Dziendziel, M. Freeman, N.. Choudhury, E. Langlois,
S. Dakshina Murthy, I. Bhat, R. Gutmann

July 1995

DISTRIBUTION OF THIS DOCUMENT IS UNLIMITED MASTER

NOTICE

This report was prepared as an account of work sponsored by the United States Government. Neither the United States, nor the United States Department of Energy, nor any of their employees, nor any of their contractors, subcontractors, or their employees, makes any warranty, express or implied, or assumes any legal liability or responsibility for the accuracy, completeness or usefulness of any information, apparatus, product or process disclosed, or represents that its use would not infringe privately owned rights.

KAPL ATOMIC POWER LABORATORY SCHENECTADY, NEW YORK 12301

Operated for the U. S. Department of Energy
by KAPL, Inc. a Lockheed Martin company

DISCLAIMER

This report was prepared as an account of work sponsored by an agency of the United States Government. Neither the United States Government nor any agency thereof, nor any of their employees, make any warranty, express or implied, or assumes any legal liability or responsibility for the accuracy, completeness, or usefulness of any information, apparatus, product, or process disclosed, or represents that its use would not infringe privately owned rights. Reference herein to any specific commercial product, process, or service by trade name, trademark, manufacturer, or otherwise does not necessarily constitute or imply its endorsement, recommendation, or favoring by the United States Government or any agency thereof. The views and opinions of authors expressed herein do not necessarily state or reflect those of the United States Government or any agency thereof.

DISCLAIMER

Portions of this document may be illegible in electronic image products. Images are produced from the best available original document.

Characteristics of Indium Oxide Plasma Filters Deposited by Atmospheric Pressure CVD

E. Langlois, S. Dakshina Murthy, I. Bhat and R. Gutmann
ECSE Department and Center for Integrated Electronics & Electronic Manufacturing,
Rensselaer Polytechnic Institute, Troy, NY 12180-3590
and
E. Brown, R. Dziendziel, M. Freeman and N. Choudhury
Lockheed-Martin, Schenectady, NY 12301

Abstract

Thin films of undoped and tin-doped In_2O_3 are being investigated for use as plasma filters in spectral control applications for thermal photovoltaic cells. These films are required to exhibit high reflectance at wavelengths longer than the plasma wavelength λ_p , high transmittance at wavelengths shorter than λ_p and low absorption throughout the spectrum. Both types of films were grown via atmospheric pressure chemical vapor deposition (APCVD) on Si (100) and fused silica substrates using trimethylindium (TMI), tetraethyltin (TET), and oxygen as the precursors. Fourier Transform InfraRed (FTIR) spectroscopy was used to measure the filter transmittance and reflectance between 1.8-20µm. Nominal conditions used during the growth of undoped In_2O_3 were a substrate temperature of 450°C and partial pressures of 1.4×10^{-4}atm. and 1×10^{-3}atm. for TMI and O_2 respectively. The O_2/TMI partial pressure ratio and substrate temperature were systematically varied to control the filter characteristics. The plasma wavelength λ_p was found to be a sensitive function of these parameters. Post-growth annealing of the films was done in inert as well as air ambient at elevated temperatures, but was found to have no beneficial effect. Tin-doped In_2O_3 was grown under similar conditions as above, with a typical TET partial pressure of 4×10^{-6}atm. Here also, the material properties and consequently the optical response were found to be strongly dependent on growth conditions such as O_2 and TET partial pressures. Both undoped and tin-doped In_2O_3 grown on fused silica exhibited enhanced transmittance due to the close matching of refractive indices of In_2O_3 and silica. X-ray diffractometer measurements indicated that all these films were polycrystalline and highly textured towards the (111) direction. The best undoped and tin-doped In_2O_3 films had a λ_p around 2.7µm, peak reflectance greater than 75% and residual absorption below 20%. These results indicate the promise of undoped and tin-doped In_2O_3 as a material for plasma filters.

Introduction

Photovoltaic (solar) cells are widely used to convert light energy from the sun into usable electrical energy through a direct conversion process. A similar device, the thermal photovoltaic cell or TPV cell, utilizes energy from the near infra-red spectrum to excite charge carriers and create electrical energy. These devices have immense practical value for generating power from thermal radiation sources. In this case, only those wavelengths corresponding to energies equal to or greater than the band gap of the TPV cell material are of use. However, the thermal source radiates energy at a continuum of wavelengths corresponding to black-body radiation. All radiation below the bandgap energy would pass through the cell and be wasted. To increase efficiency, wavelengths corresponding to sub band gap energies should be reflected back into the source in order to reduce the input power to the system. This spectral control technique can be accomplished utilizing a heavily doped semiconductor filter or "plasma filter". These filters have already been developed for use in efficient incandescent and sodium-vapor lamps, solar collectors and energy-efficient windows for houses[1-2]. However, these applications require the transmission of radiation in the visible spectrum while reflecting back all infra-red radiation. For use in TPV cells, the filters need to transmit wavelengths shorter than about 2.5μm and reflect all longer wavelengths.

This requirement calls for the use of a highly conductive material with a large enough bandgap whose carrier concentration can be controlled to obtain the required behavior. Transparent conducting oxides such as indium tin oxide or indium oxide are well suited for this purpose[1-2]. These films have been synthesized by various methods such as thermal evaporation[3], electron beam evaporation[4], rf magnetron sputtering[5], dc magnetron sputtering[6], ion beam sputtering[7], spray pyrolysis[8], chemical vapor deposition[9] and pulsed laser deposition[10]. These techniques have concentrated on the growth of material transparent to visible light but not to infrared. The optical and electrical properties of these materials have also been well documented[11-12]. In general, these methods are used to obtain materials with as high a carrier concentration as possible. However, for TPV applications, it is necessary to tune the "plasma wavelength" of the filter between 2.5-3μm, which requires a finer control of the carrier concentration in the material. We chose to use atmospheric pressure chemical vapor deposition as the growth technique. The use of carefully controlled proportions of the highly pure organometallic reactants allows us to easily regulate the carrier concentration to the required value without resorting to post growth annealing techniques. Also, the use of high deposition temperatures and a chemical

vapor deposition technique ensures the growth of inherently good starting material. Another point to note is that the amount of tin incorporated in indium tin oxide layers grown by the other techniques mentioned above (~5%) is higher than we intend to use in our tin-doped layers.

This paper focuses on the development of an In_2O_3 plasma filter for use in TPV spectral control applications. The growth and characterization of thin layers of undoped and tin-doped In_2O_3 used as plasma filters is described below. The principle behind the operation of these plasma filters is also explained in brief.

Technical Background

Indium oxide is a solid which most commonly occurs as the sesquioxide, In_2O_3. As reported in the literature[13], In_2O_3 is a polycrystalline solid with a cubic unit cell structure whose lattice parameter a_0=10.117Å . The structure of In_2O_3 is related to that of the fluorite structure, from which it can be derived by removing one-quarter of the anions[13].

There are two types of In_2O_3 plasma filters under consideration in this paper. The first type, commonly referred to as "undoped" Indium Oxide is in fact doped by oxygen vacancy defects, which are always present as a consequence of the growth process. In_2O_3 is an ionic solid consisting of indium cations (In^{3+}) and oxygen anions (O^{2-}). When an oxygen atom is removed from the normal crystal site, two electrons are left in the vacancy. One or both of these electrons may be excited into the conduction band leaving behind a single or doubly charged vacancy. The presence of these electrons in the conduction band the turns the undoped In_2O_3 into an n-type conducting material. This behavior may be described as follows[14]:

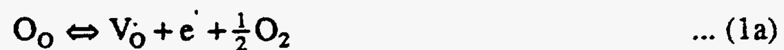

$$O_O \Leftrightarrow V_O^{\cdot} + e^{'} + \tfrac{1}{2}O_2 \qquad \text{... (1a)}$$

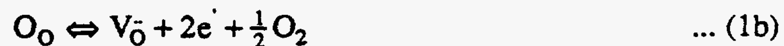

$$O_O \Leftrightarrow V_O^{\cdot\cdot} + 2e^{'} + \tfrac{1}{2}O_2 \qquad \text{... (1b)}$$

where V ≡ vacancy
O ≡ oxygen
e ≡ electron
ö / e' ≡ effective / actual charge

The second type of In_2O_3 is the tin-doped In_2O_3 which is extrinsically doped by tin atoms. Tin is a tetravalent atom and becomes a Sn^{4+} cation when fully ionized. If tin is incorporated into an indium (In^{3+}) site, an extra electron is removed to the conduction band leaving behind a positive effective charge. Tin thus behaves as a donor making tin-doped In_2O_3 also an n-type conducting material.

In both types of In_2O_3, the aim is to obtain n-type material with a very high concentration of electrons obtained from the donors. The high carrier concentration is the basis for the working of the plasma filter, which has to do with the collective oscillations of the "plasma" formed by the negatively charged electrons and the positively charged donors. At a particular wavelength of oscillation corresponding to the resonant case, known as the plasma wavelength λ_P, the material undergoes a transition such that at wavelengths $\lambda > \lambda_P$ it is highly reflective and for $\lambda < \lambda_P$ it is highly transmissive in nature. By definition, λ_p is defined as the wavelength where the real part of the refractive index, n, is equal to the complex part, k. λ_p is given by the following equation[1]:

$$\lambda_P = 2\pi c_o \left(\frac{nq^2}{\varepsilon_o \varepsilon_r m^*} - \gamma^2 \right)^{-1/2} \qquad ...(2)$$

where c_o = speed of light in free space

n = charge carrier concentration

ε_o = permittivity of free space

ε_r = relative dielectric constant of medium

m^* = effective mass of charge carriers

γ = the damping rate

q = electronic charge

In eq.(2), γ^2 , which depends on the mobility μ of the electrons is usually quite small compared to the other term and may be neglected. However, the mobility μ does affect the steepness of the reflectance and transmittance curves in the transition region [1].

For our case, the goal is to position λ_P such that shorter wavelengths ($\lambda < \lambda_p$) will be those usable by the TPV cell and longer wavelengths ($\lambda > \lambda_p$) will be reflected back into the source. A nominal λ_p of 2.7μm is chosen for application for a cell with a bandgap around 0.55eV. It is also necessary to make the reflectance and transmittance curves close to unity in their dominating regions and to make them as steep in the transition region as possible. The absorption by the filter also needs to be minimized. This calls for good

control of the charge carrier concentration and making the mobility as high as possible to maximize the obtainable power and efficiency of the TPV cell.

Experimental procedure

1) *Substrate preparation*

The substrates used for the deposition of indium oxide were <100> oriented p-type Si. High resistivity wafers were used, doped to a nominal resistivity of 30 Ωcm in order to minimize free-carrier absorption in the bulk of the wafer. Fused silica substrates, 1mm thick, were also used for some runs. The 1" square Si substrates were immersed in beakers containing trichloroethane (TCA), which were placed in an ultrasonic bath for 2-3 minutes and then transferred to a hot plate for approximately 3 minutes. The wafers were rinsed off with acetone followed by methanol. The cleaning in TCA removes organic contaminants and particulates from the surface and the rinsing steps remove any organic residues left by the TCA. A final dilute HF dip for 30 seconds was performed to etch away the native oxide layer on the Si surface. A similar procedure was used to clean the fused silica substrates, omitting the dilute HF dip. The substrates were then immediately transferred to the growth chamber.

2) *Chemical vapor deposition system*

All growth runs of indium oxide or tin doped indium oxide were carried out in an atmospheric pressure CVD system. The system consists of a pyrex chamber, a resistively heated susceptor, a glass funnel, and 316SS steel plumbing connecting the chamber to the trimethylindium / tetraethyltin bubblers and to the argon / oxygen tanks. The organometallic indium and tin precursors enter the chamber through the funnel while the oxygen inlet is at the side. This ensures that the reaction occurs at the susceptor, reducing the possibility of gas-phase reactions. Gas flows are controlled using flow meter tubes (a mass flow controller was used for tetraethyltin). A diagram of the CVD system chamber is shown in figure 1.

3) *Growth Procedure*

Growth runs were initiated by flushing all gas lines with ultra-high purity argon. Under a constant flow of 1slpm of argon, the wafer was inserted into the chamber through the inlet port and positioned directly under the glass funnel. The chamber was flushed for

10 minutes with 5 slpm of argon to purge the system of oxygen. Immediately afterwards, the wafer was heated by the susceptor to the growth temperature, typically 450^0C.

Precursors used for growing indium oxide or tin doped indium oxide were trimethylindium, tetraethyltin, and extra-dry grade of O_2. Ultra-high purity argon was used as a carrier gas at a total flow of approximately 5 slpm. Reactant flows were started simultaneously at low flows of trimethylindium (75 sccm of Ar was flowed initially through the bubbler) which was subsequently raised to the normal flow rate (300 sccm of Ar through the bubbler) after about ten minutes of growth. This was done to promote uniform nucleation over the wafer surface by growing the initial layer slowly and avoiding the formation of indium droplets caused by excess indium. To achieve a layer thickness of about 0.7 to 0.8 μm, a total growth time of about 65 minutes was necessary. The growth was monitored periodically by observing the color changes due to constructive interference as the film thickness increased. These color changes were then correlated with the thickness values on a color chart. This monitoring helped to observe changes in the growth rate and provided an approximate method for determining when the growth run should be terminated.

An optimum funnel height of 4 cm above the wafer surface was established by trial and error. This was chosen to minimize the possibility of poor nucleation caused by an indium rich surface while maintaining a reasonable growth rate. It was found to be necessary to periodically clean the reaction chamber to prevent dusting of the substrate surface. The procedure detailed above was used for the growth of all the layers discussed below. Systematic variations in growth conditions were used to control the optical properties of the filters.

4) *Characterization*

Reflectance and transmittance measurements over a spectral range of 1.8-20μm were carried out using a Fourier Transform InfraRed (FTIR) spectrometer. Structural characterization was carried out using a Philips X-Ray diffractometer using Cu Kα radiation. Hall effect measurements were also done to extract electrical properties such as mobility and carrier concentration. However, owing to the highly conducting nature of these films, the parameters extracted from the Hall measurements were not very reliable. Thickness measurements on the films were done using a spectroscopic ellipsometer with a spectral range of 400-740 nm (J. A.Woollam Co.) and also an α-step profilometer.

Experimental Results and Discussion

A number of different studies were carried out on undoped and tin-doped In_2O_3 plasma filters by varying various growth conditions, post-growth treatments and substrates used. Unless explicitly mentioned, the growth temperature was 450°C for all cases. The layers were all grown to a final thickness of about 0.65-0.85μm, which corresponds to the skin depth for absorption of near infrared waves incident on these films.

1) *Undoped Indium Oxide*

a) Effect of varying O_2/TMI partial pressure ratio

A very effective method for controlling the carrier concentration and consequently the λ_p in undoped indium oxide was to vary the O_2/TMI partial pressure ratio. A constant partial pressure of 1.4×10^{-4}atm of TMI (corresponding to a flow of 300 sccm through the bubbler) was maintained and the oxygen partial pressure was varied in different runs from 8×10^{-4}atm to 1.5×10^{-3} atm. The growth temperature was maintained at 450°C. The results of these studies are shown in fig.2. We see that λ_p increases with a rise in the O_2 partial pressure. The native oxygen vacancy concentration is expected to fall at higher partial pressures of O_2, as this would lead to a more stoichiometric material. This drop in vacancy concentration results in a smaller value for the carrier concentration and consequently a larger λ_p. As we can see from eq (2), λ_p is a sensitive function of the carrier concentration and thus small changes in the O_2 partial pressure cause large shifts in λ_p over the range of interest.

b) Effect of varying the growth temperature

Initially, growth of undoped In_2O_3 was carried out at a susceptor temperature of 350°C. Reasonably good optical characteristics were obtained, but the growth rate was found to be very low. In order to increase the growth rate and optimize the optical properties of the film, a series of growth runs were made at temperatures of 400, 450, and 500°C. Here, the partial pressures of TMI and O_2 were maintained constant at 1.4×10^{-4}atm and 1×10^{-3}atm respectively. As seen in figure 3, there is an increase in λ_p as the growth temperature is raised. This indicates that the oxygen vacancy concentration drops at higher growth temperatures, which can be

attributed to improved stoichiometry of the film. It appears that the reaction between the indium and oxygen species is more favored at higher temperatures. In short, this provides yet another method of effectively controlling λ_p. Growth at temperatures higher than 500°C was not investigated because of potential problems with increased recirculation and gas-phase reactions, leading to dusting and poor surface morphology.

c) Effect of using fused silica as the substrate material

Fused silica was used as an alternate substrate upon which to grow In_2O_3. The growth was carried out on Si and fused silica substrates at 450°C, under partial pressures of 1.4×10^{-4} atm for TMI and 1×10^{-3}atm for O_2. As we can see from the reflectance and transmittance spectra of figs.4&5, λ_p is nearly the same on both substrates. However, for the In_2O_3 grown on fused silica, the transmittance is greatly improved and is as high as 80% at a wavelength of 2 μm (see figure 5). This is a result of the smaller difference in refractive indices of In_2O_3 (n = 2) and fused silica. The refractive index n = 1.45 for fused silica and n = 3.5 for silicon. This also explains the absence of the interference fringe in the reflectance for $\lambda < \lambda_p$. The interesting feature of this study was that similar material was grown on both Si (100), which is a crystalline substrate and fused silica, which is amorphous. The substrate does not seem to have a significant effect on the growth of undoped In_2O_3. It is likely that the surface of Si is covered by a thin native oxide layer prior to the growth, so that the differences between Si and silica are not significant.

d) Annealing Studies

It has been reported in the literature that post-deposition annealing of indium oxide samples grown by other techniques has helped improve their optical and electrical properties[15-17]. However, we discovered that this was not the case for our CVD grown samples. Rapid thermal annealing was carried out in a N_2 ambient at 850^{0}C for 5 min. and 1050^{0}C for 20 seconds and the results are shown in figures 6 and 7 respectively. Figure 8 shows the reflectance spectrum of a sample annealed in an air ambient at 750^{0}C for 5 hours. We can see that annealing in the inert N_2 ambient resulted in a shift of λ_p to lower wavelengths, probably caused by loss of oxygen from the sample, resulting in an increase in the carrier concentration. On the other hand, annealing in an air ambient had the effect of shifting λ_p to longer wavelengths. This may be a consequence of O_2 from the ambient diffusing in and reducing the vacancy concentration. In both cases, *no* beneficial effect was

observed upon annealing, in stark contrast to studies by other workers[15-17]. This can be attributed to the fact that our material was grown by CVD at a relatively high temperature, which promotes the growth of good stoichiometric polycrystalline material, without the presence of a second phase such as excess indium droplets. The In_2O_3 used by other workers was grown by techniques such as sputtering and reactive evaporation, which yield inherently poorer starting material that is far more amenable to improvement upon appropriate annealing.

e) X-ray Studies

X-ray measurements were carried out using a diffractometer in order to study the degree of crystallinity in the In_2O_3 samples. A typical x-ray diffraction spectra of a In_2O_3 / Si sample is shown in figure 9. A large number of peaks were obtained with good intensity on all samples, indicating that the In_2O_3 was polycrystalline. On comparison with standard powder diffraction data for In_2O_3, the strong (222) peak showed evidence of high texture in the <111> direction, which agrees with results obtained by other workers on In_2O_3 grown by chemical vapor deposition[9]. No significant changes were observed in the relative intensities of the various peaks for measurements on samples grown under a variety of different growth conditions mentioned above. It is also interesting that the x-ray measurements done on indium oxide samples grown on fused silica also exhibit a high degree of texturing in the <111> direction. This shows that the growth temperature is high enough to ensure that the reactant species have enough surface mobility in order to form large grains oriented in a particular direction, irrespective of the substrate material.

2) *Tin Doped Indium Oxide*

As seen before (Fig. 4&5), good results were obtained with the undoped In_2O_3. However, the transition of the reflectance curve for $\lambda > \lambda_p$ was not as sharp as desired. The absorption also needed to be reduced further. In undoped In_2O_3, the n-type doping arises from the native defects (see eq.1), which in turn depends on the oxygen partial pressure during the growth. The oxygen partial pressure has to be kept low during the growth in order to achieve the high carrier concentrations required for these filters. However, the growth of a good film with better surface morphology requires a higher flow of oxygen. In fact, we use a larger O_2 / TMI partial pressure ratio at the beginning of the growth in order to obtain a good nucleation layer without the formation of In droplets. The conflicting requirements

mentioned above can be addressed by the use of Sn as an extrinsic dopant. In tin doped films, we can adjust the flow of the Sn precursor to obtain a primary control of the carrier concentration whereas the oxygen flow can be adjusted to optimize the film stoichiometry and morphology. This may lead to reduced scattering in the films and consequently higher mobility, resulting in a sharper transition of the reflectance spectra.

a) Effect of varying TET partial pressure

The tin doping was carried out using very low partial pressures of TET. These ranged from 1-4% of the TMI partial pressure in the *gas phase*. We cannot expect the same ratio for the actual incorporation of Sn and In as the reactivity of TET with O_2 is very low. At percentages less than 2%, no significant change was observed either in the reflectance curve or the position of λ_p, indicating that a negligible amount of active Sn was incorporated as compared to the oxygen vacancies. However, when the tin percentage was increased from 2% to 4%, the result was quite striking (fig. 10). Here, partial pressures of O_2 and TMI were kept constant at 3×10^{-3} atm and 1.4×10^{-4} atm respectively, while the partial pressure of TET was varied from 2.8×10^{-6} atm. to 5.6×10^{-6} atm. Note that the O_2 partial pressure is maintained at a significantly higher level than for the undoped In_2O_3 films in order to improve the film quality.

Fig.11 sums up the results of varying the tin doping at constant TMI and O_2 partial pressures. Here, the carrier concentrations calculated from eq(2) for λ_p (assuming λ_p to be the minimum of the FTIR reflectance spectrum) have been plotted vs. partial pressures of TET at a constant flow of 15 sccm of O_2 (3×10^{-3} atm). The result indicates that increasing the tin doping results in a direct increase in the carrier concentration. This is yet another way in which to control the position of λ_p around the required value.

b) Effect of varying O_2 partial pressure

Since the carrier concentration in these films was found to be primarily controlled by the Sn precursor partial pressure, the oxygen flow may be varied in order to optimize the crystalline and optical properties. Varying the O_2 partial pressure might also provide a means of separating the contributions from the tin and the O vacancies to the carrier concentration. A series of growth runs were carried out at various partial pressures of O_2 ranging from 3×10^{-3} atm. to 7.2×10^{-3} atm while

keeping the partial pressures of TMI and TET constant at 1.4×10^{-4}atm and 3.93×10^{-6}atm respectively. As can be seen from fig.12, increasing the O_2 flow resulted in λ_p shifting to lower wavelengths. We would expect that the native oxygen defect concentration would fall as the O_2 partial pressure were increased. If the same amount of tin were incorporated in all cases, the carrier concentration should not have been affected by varying O_2. The observed increase in the carrier concentration seems to indicate that tin incorporation is favored at higher O_2 partial pressures. Fig. 13 summarizes the results of this study, where the carrier concentration calculated from λ_p (as above) is plotted versus O_2 partial pressure.

c) Effect of using fused silica as an alternative to silicon (100)

Good results were obtained with the tin-doped In_2O_3 grown on Si. Figure 14 shows the transmittance and reflectance spectrum for the best tin-doped In_2O_3 layer grown on Si. The partial pressures of O_2, TMI and TET used were 1×10^{-3}atm, 1.4×10^{-4}atm and 2.8×10^{-6}atm respectively. It was decided to use fused silica as a substrate to take advantage of the increased transmittance observed previously for undoped In_2O_3 grown on silica..

Fused silica was used as an alternative to Si (100) on which to grow tin doped In_2O_3. As in the case of undoped In_2O_3 growth on silica, we found that the material was essentially the same as that grown on Si (100). However, as expected, the reflectance and transmittance spectra were quite different owing to the different optical properties of the substrate material. Fig. 15 shows the reflectance and transmittance spectra for tin-doped In_2O_3 grown on fused silica under partial pressures for O_2, TMI and TET being 3×10^{-3} atm, 1.4×10^{-4} atm and 5.4×10^{-6} atm respectively. We clearly observe the higher transmittance for $\lambda < \lambda_p$ compared to figure 14. λ_p is shifted to a low value of nearly 2μm, but the enhanced transmission makes up for the low value of λ_p. The act of shifting λ_p to a low value also has the beneficial effect of raising the reflectance at high wavelengths. The dip in transmission at 2.74μm is due to the substrate. The sharp dip in transmittance above 4μm is again due to the property of the fused silica. This tin doped In_2O_3 film exhibits high transmittance and reflectance in the required regions with low absorption and is one of the best filters grown in the course of this work.

d) Effect of varying layer thickness:

As mentioned before, the layers grown in this study had thicknesses ranging from 0.65-0.85μm. This was chosen on the basis of the skin depth for the wavelengths of interest. We would expect to get a sharper transition in the reflectance for thicker layers owing to the larger depth of the plasma through which the wave has to pass before being transmitted through the substrate. On the other hand, the very same reason would lead to an increase in absorption, degrading the filter optical properties. To observe the effect of these conflicting mechanisms, a tin-doped In_2O_3 layer was grown at twice the usual thickness. Partial pressures for O_2, TMI and TET were 3×10^{-3} atm, 1.4×10^{-4} atm and 2.8×10^{-6} atm respectively. As can be seen from fig. 16, the reflectance does improve compared to that of a layer grown to the usual thickness (fig.14) with a very sharp transition for $\lambda > \lambda_p$. The larger thickness also leads to the presence of interference oscillations in the reflectance for $\lambda < \lambda_p$. However, the absorption is much higher, leading to a bigger dip in the transmittance at λ_p and a significant decrease in the transmittance for $\lambda < \lambda_p$.

e) X-ray studies

X-ray diffractometer measurements were done as described before. Figure17 shows the x-ray diffraction data for a sample of tin-doped In_2O_3 grown on Si. The results indicate that the tin-doped In_2O_3 was also polycrystalline with a <111> texture, similar to the result obtained on undoped In_2O_3. Also, as reported by other workers[13], there was no evidence of a separate SnO_2 peak owing to the high solubility of Sn in the In_2O_3 lattice. These workers also observed that the incorporation of tin in reasonable amounts (~10%) results in an appreciable shift in the peak positions from the undoped to the tin-doped layer. However, we did not observe any noticeable shift in the peak positions of the x-ray diffraction data between undoped and tin-doped In_2O_3. This result suggests that a very small amount of tin (< 1%) was actually incorporated into the lattice, which is not unreasonable since we would expect the incorporation of tin during chemical vapor deposition using a relatively stable species such as TET to be quite low. We intend to confirm this hypothesis by carrying out Secondary Ion Mass Spectrometry (SIMS) on our samples.

Summary and Conclusion

From our results, we see that there are two principal methods of controlling the carrier concentration and consequently λ_p in our plasma filters. The first method is to control the native oxygen vacancy concentration by suitably adjusting the TMI / O_2 partial pressure ratio to obtain the required amount of oxygen vacancy donors. Good results were obtained with this, although in practice it is very difficult to reproducibly control the stoichiometry of the In_2O_3 as well as the surface morphology of the films.

We can also extrinsically dope the indium oxide with tin. This provides us with a more direct method of controlling the carrier concentration, and is easier to control. As discussed earlier, the material grown using tin doping may exhibit better optical properties through improvement in crystalline quality. Figs. 4&15 show the results for the best undoped and tin-doped plasma filters. We can see that the absorption is lower and the reflectance higher for the tin-doped material.

Varying the growth temperature is yet another way of shifting λ_p. However, this is not a good technique as low temperatures lead to low growth rates and high temperatures increase the chance of gas-phase reactions. A susceptor temperature of 450°C was found to be appropriate for our system.

Despite the successful results which other researchers have had on post-growth annealing of In_2O_3, annealing seems to be either detrimental or ineffective for our CVD grown filters. This may be attributed to the good inherent crystalline quality obtained directly by CVD techniques.

The choice of substrate does have a significant effect on the optical properties of the plasma filters. X-Ray studies indicate that the same type of <111> oriented polycrystalline material is grown on both substrates. Thus, the change in the filter optical response arises from the optical properties of the substrate material. As expected, the lower refractive index of fused silica results in a much improved transmittance for $\lambda < \lambda_p$. The higher transmittance allows us to shift λ_p to wavelengths as low as 2μm, resulting in an improvement in reflectance at longer wavelengths (fig.15).

At present, the results on In_2O_3 are very promising but a number of improvements are needed before the filters can be successfully implemented on TPV cells. The uniformity and reproducibility of the layers need to be improved. Changes may be required to the system configuration in order to achieve this. It is also necessary to arrive at an optimum

set of growth parameters in terms of reactor conditions, growth time etc. to obtain the best possible response.

The above results indicate that undoped and tin-doped In_2O_3 material is well suited for use as a spectral control filter used in TPV applications.

Acknowledgement

The authors wish to thank J. Barthel for technical assistance.

List of Figures

Fig. 1 Schematic diagram of the Chemical Vapor Deposition system.

Fig. 2 Variation of λ_p with O_2 partial pressure used for the growth of undoped In_2O_3 on Si. (TMI partial pressure kept constant at 1.4×10^{-4}atm).

Fig. 3 Variation of λ_p with the growth temperature used for undoped In_2O_3 growth on Si. (Partial pressures of TMI and O_2 kept constant at 1.4×10^{-4}atm and 1×10^{-3}atm respectively).

Fig. 4 Reflectance and transmittance spectra of undoped In_2O_3 grown on Si (100). The absorption is less than 25%.

Fig. 5 Reflectance and transmittance spectra of undoped In_2O_3 grown on fused silica.

Fig. 6 Reflectance spectra of undoped In_2O_3 annealed at 850°C for 5 min. (RTA) in N_2.

Fig. 7 Reflectance spectra of undoped In_2O_3 annealed at 1050°C for 20 sec (RTA) in N_2.

Fig. 8 Reflectance spectra of undoped In_2O_3 annealed in air ambient at 750°C for 5 hours.

Fig. 9 Results of X-ray diffraction measurement on undoped In_2O_3 (Cu Kα radiation).

Fig.10 Variation of λ_p with TET partial pressure used during the growth of tin-doped In_2O_3. (Partial pressures of TMI and O_2 were kept constant at 1×10^{-4}atm and 3×10^{-3}atm respectively)

Fig. 11 Carrier concentration of tin-doped In_2O_3 layers vs. partial pressure of TET used during the growth.

Fig. 12 Variation of λ_p with O_2 partial pressure used during the growth of tin-doped In_2O_3. (Partial pressures of TMI and TET were kept constant at 1×10^{-4}atm and 3.93×10^{-6}atm respectively).

Fig. 13 Carrier concentration of tin-doped In_2O_3 layers vs. partial pressure of O_2 used during the growth.

Fig. 14 Reflectance and transmittance spectra of tin-doped In_2O_3 grown on Si (100).

Fig. 15 Reflectance and transmittance spectra of tin-doped In_2O_3 grown on fused silica.

Fig. 16 Reflectance and transmittance spectra of tin-doped In_2O_3 grown on Si (100) to a thickness of 1.3μm (2 × normal thickness).

Fig. 17 Results of X-ray diffraction measurement on tin-doped In_2O_3 (Cu Kα radiation).

Literature Cited

1. H. Köstlin and G. Frank, " Thin-film reflection filters " , *Philips Tech. Rev.*, 41, No.7/8 , pp. 225-238 (1983-84).
2. J.C.C. Fan and F.J. Bachner, " Transparent heat mirrors for solar-energy applications ", *Applied Optics*, 15, No.4, pp 1012-1017 (April 1976).
3. A. Subrahmanyam and N. Balasubramanian, *Semicond. Sci. Tech.*, 7, pp.324 (1992).
4. H.J. Krokoszinski and R. Oesterlein, *Thin Solid Films*, 187, pp.179 (1990).
5. M.B. Buchanan, J.B. Webb and D.F. Williams, *Appl. Phys. Lett.*, 37, pp.213 (1980).
6. S. Maniv, C.J. Miner and W.D. Westwood, *J. Vac. Sci. Tech*, A1, pp.1370 (1983).
7. J.C.C. Fan, *Appl. Phys. Lett.*, 34,pp.515 (1979).
8. R. Groth, *Phys. Status. Solidi*, 14, pp.69 (1966).
9. T. Maruyama and K. Fukui, " Indium-Oxide thin films prepared by chemical vapor deposition ", *Appl. Phys. Lett.*, 70, pp.3848-3851 (1991).
10. J.P. Zheng and H.S. Kwok, " Low resistivity indium tin oxide films by pulsed laser deposition ", *Appl. Phys. Lett.*, 63, pp.1-3 (1993).
11. H. Köstlin, R. Jost and W. Lems, " Optical and electrical properties of doped In_2O_3 films ", *Phys. Status Solidi*, a29, pp.87 (1975).
12. H.K. Müller, " Electrical and optical properties of sputtered In_2O_3 films ", *Phys. Status Solidi*, 27, pp.733 (1968).
13. Ph. Parent, H. Dexpert and G. Tourillon, " Structural Study of Indium Oxide Thin Films Using X-Ray Absorption Spectroscopy and X-Ray Diffraction ", *J. Electrochem. Soc.*, 139, No. 1, pp. 277 (Jan 1992).
14. Per Knofstad, *Nonstoichiometry, Diffusion, and Electrical Conductivity in Binary Metal Oxides.*, John Wiley & Sons, Inc. New York (1972).
15. W.G. Haines and R.H. Bube, "Effects of heat-treatment on the optical and electrical properties of indium-tin oxide films ", *J. Appl. Phys.*, 49, pp.304-307 (1978).
16. K. Ito, T. Nakazawa and K. Osaki, " Amorphous-to-crystalline transition of indium oxide films deposited by reactive evaporation ", *Thin Solid Films*, 151, pp.215-222 (1987).

17. N. G. Patel and B.H. Lashkari, " Conducting transparent indium-tin oxide films by post-dpeosition annealing in different humidity environments ", *J. Material. Sci.*, 27, pp.3026-3031 (1992).

System Chamber Diagram

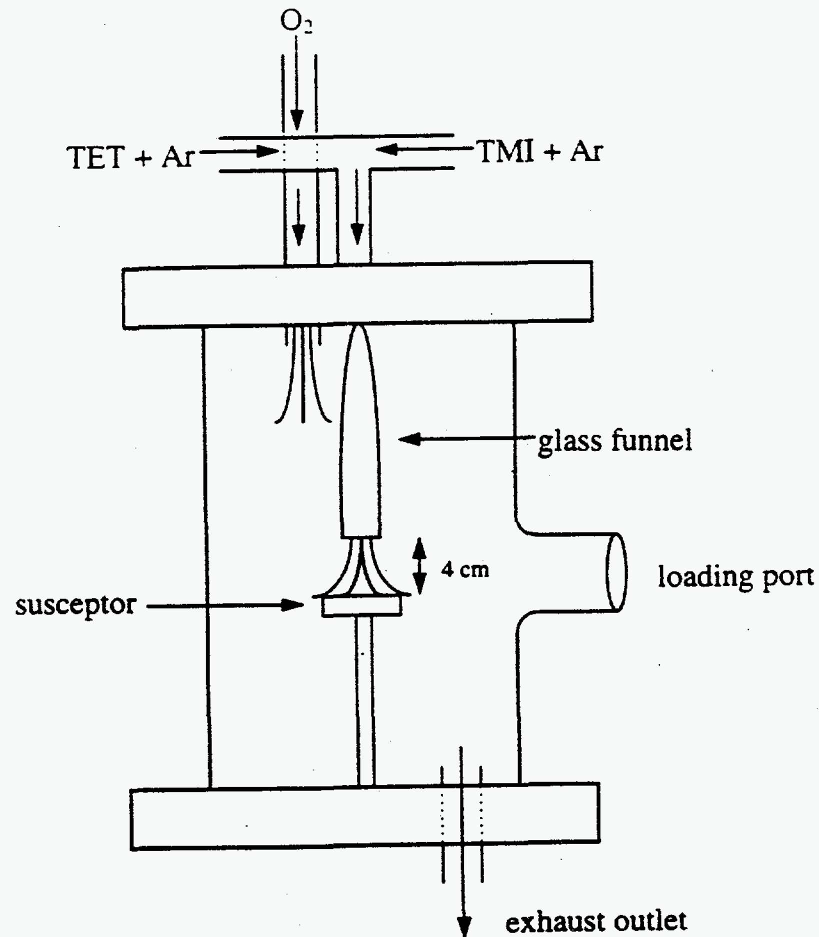

Fig. 1 Schematic diagram of the Chemical Vapor Deposition system used for the growth of undoped and tin-doped In_2O_3.

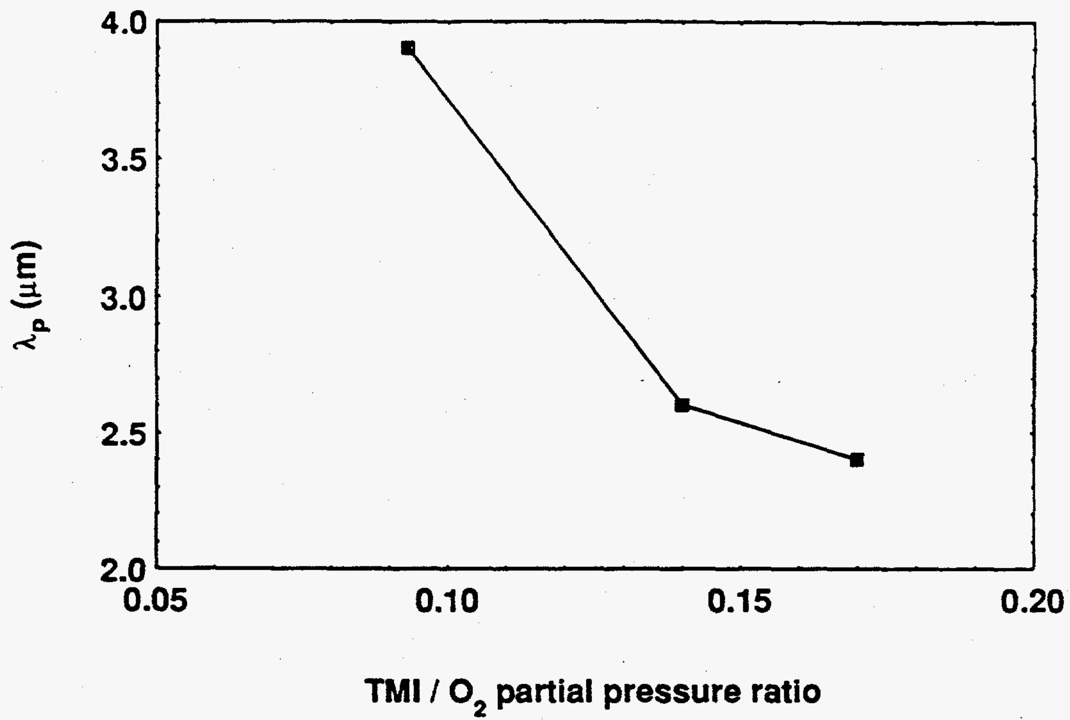

Fig. 2 Variation of λ_p with TMI / O_2 partial pressure ratio used for the growth of undoped In_2O_3 on Si. (TMI partial pressure kept constant at 1.4×10^{-4}atm).

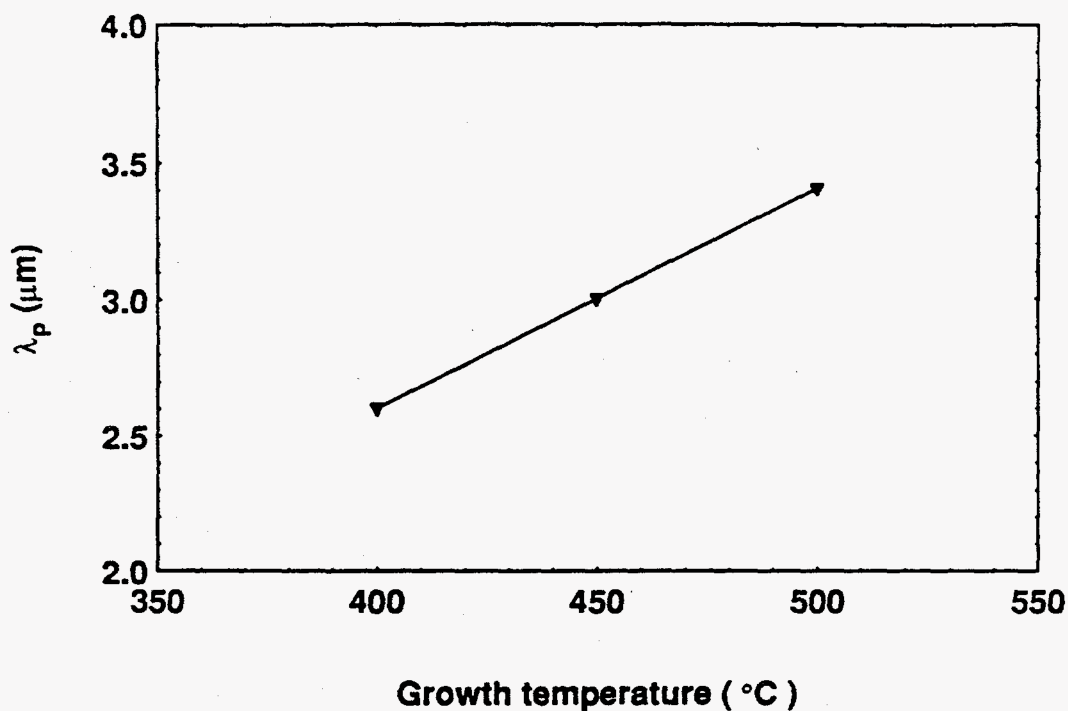

Fig. 3 Variation of λ_p with the growth temperature used for undoped In_2O_3 growth on Si. (Partial pressures of TMI and O_2 kept constant at 1.4×10^{-4}atm and 1×10^{-3}atm respectively).

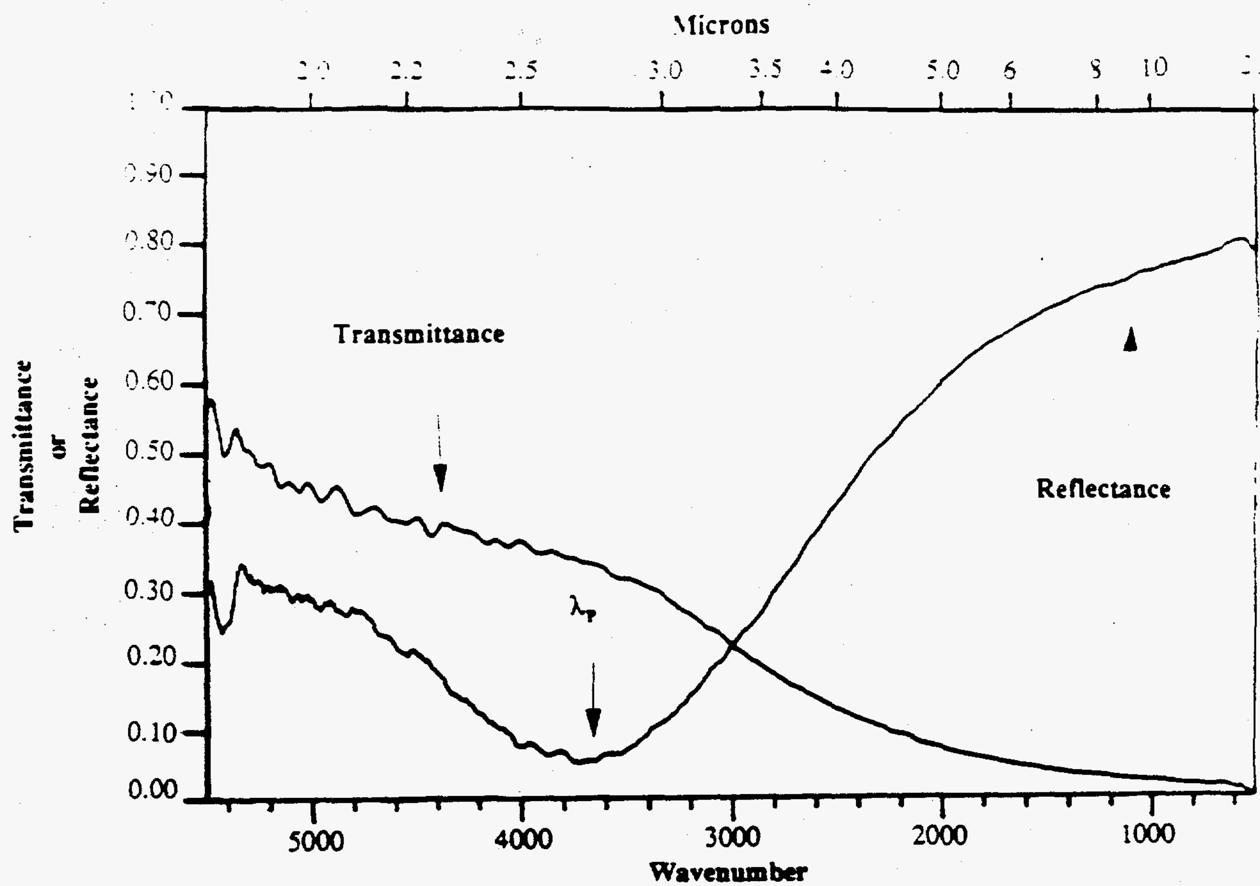

Fig. 4 Reflectance and transmittance spectra of undoped In_2O_3 grown on Si (100). The absorption is less than 25% .

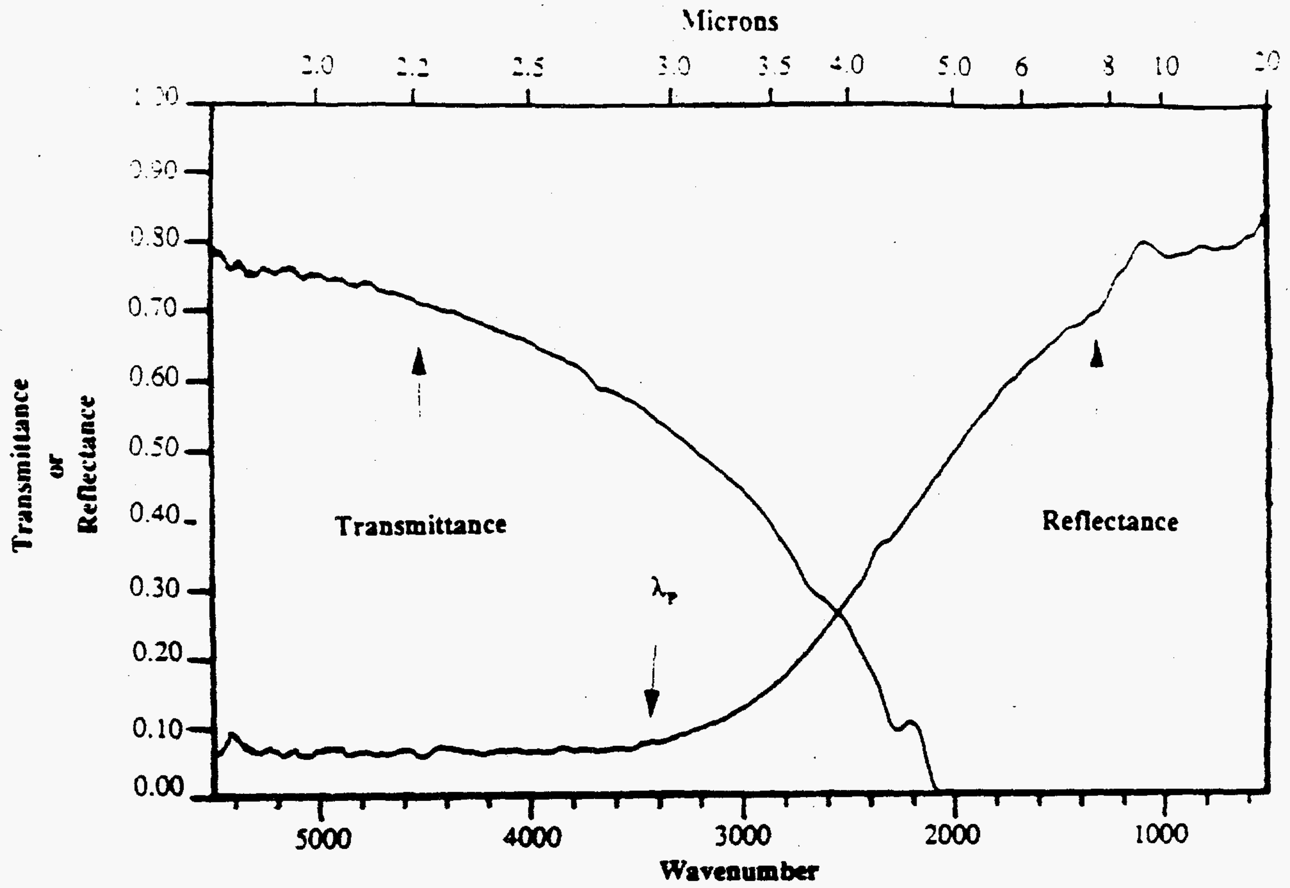

Fig. 5 Reflectance and transmittance spectra of undoped In_2O_3 grown on fused silica.

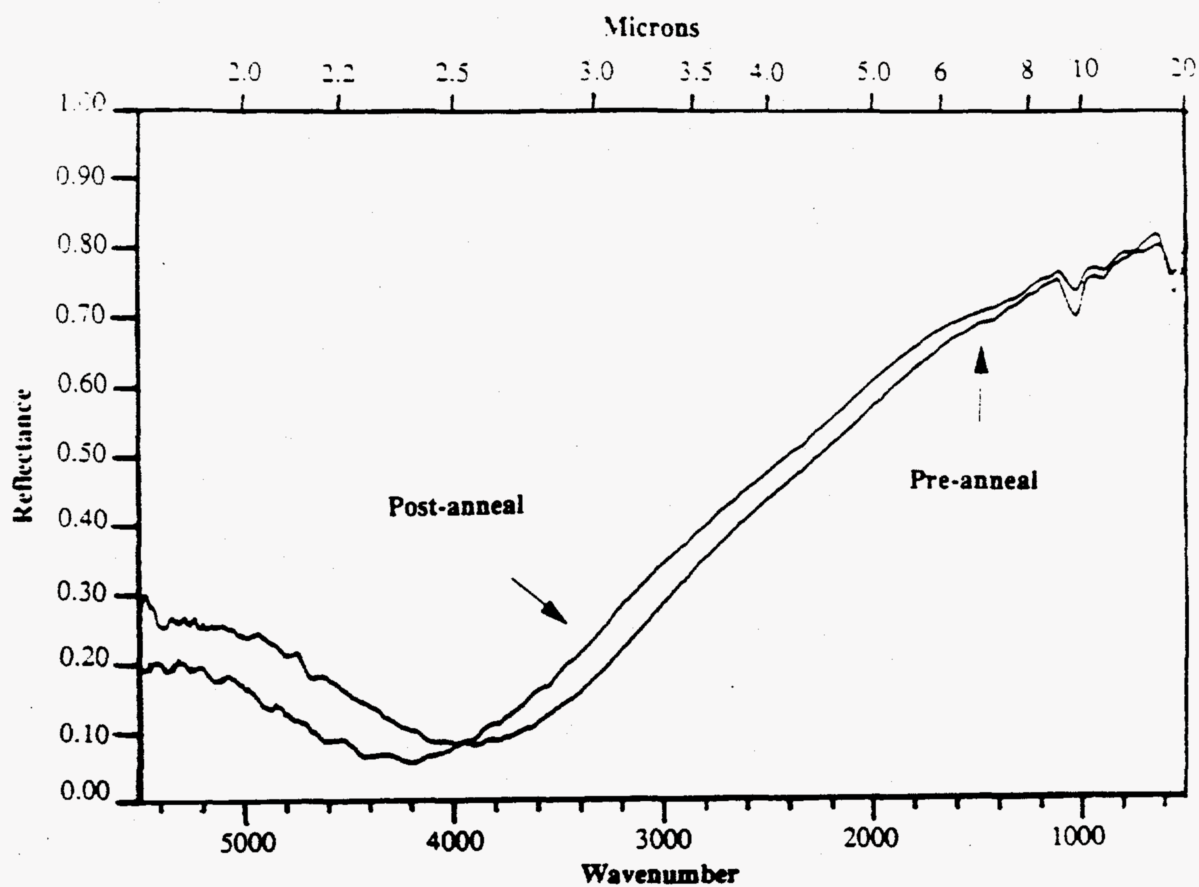

Fig. 6 Reflectance spectra of undoped In_2O_3 annealed at 850°C for 5 min. (RTA) in N_2.

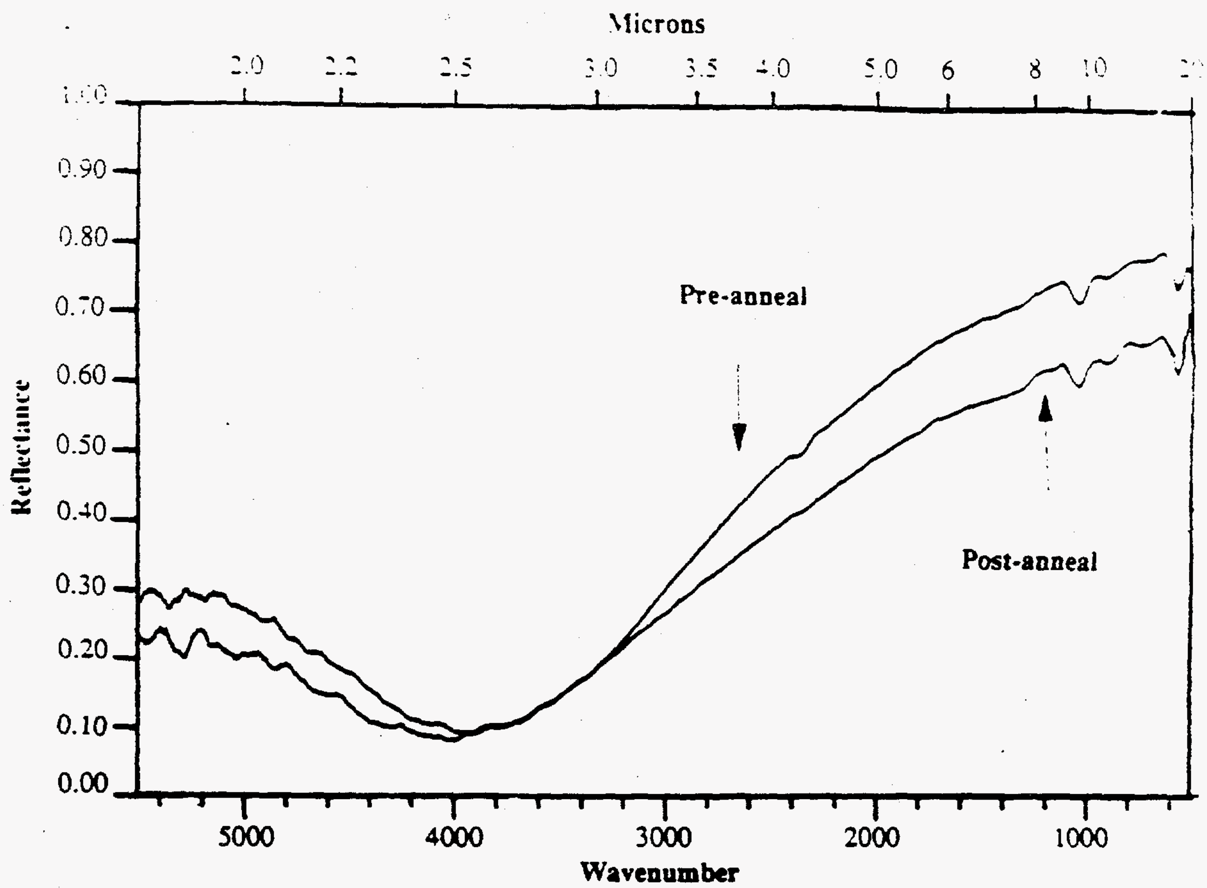

Fig. 7 Reflectance spectra of undoped In_2O_3 annealed at 1050°C for 20 sec (RTA) in N_2.

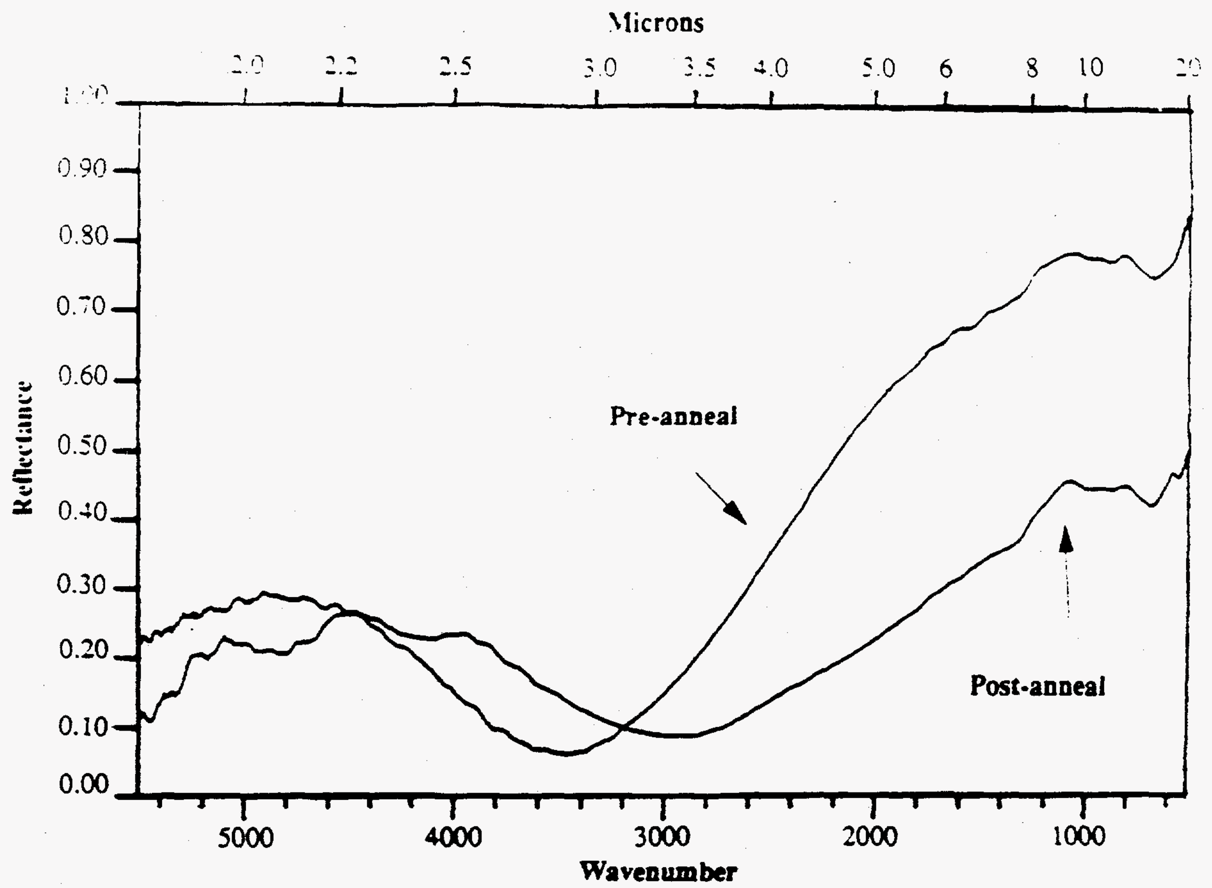

Fig. 8 Reflectance spectra of undoped In_2O_3 annealed in air ambient at 750°C for 5 hours.

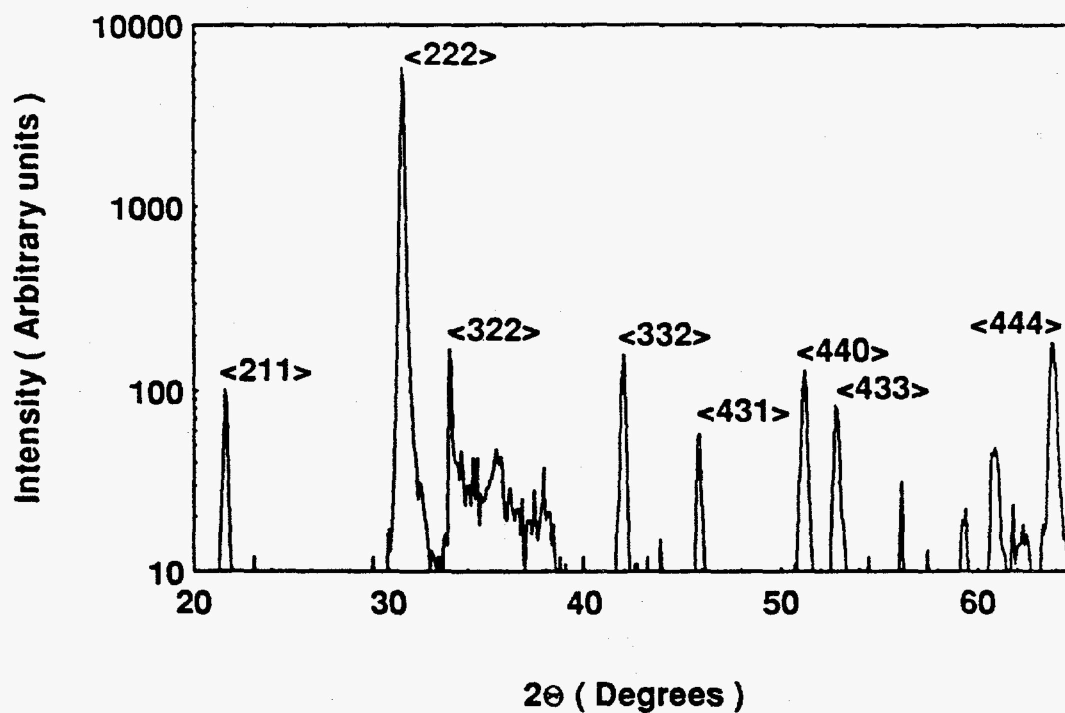

Fig. 9 Results of X-ray diffraction measurement on undoped In_2O_3 (Cu Kα radiation).

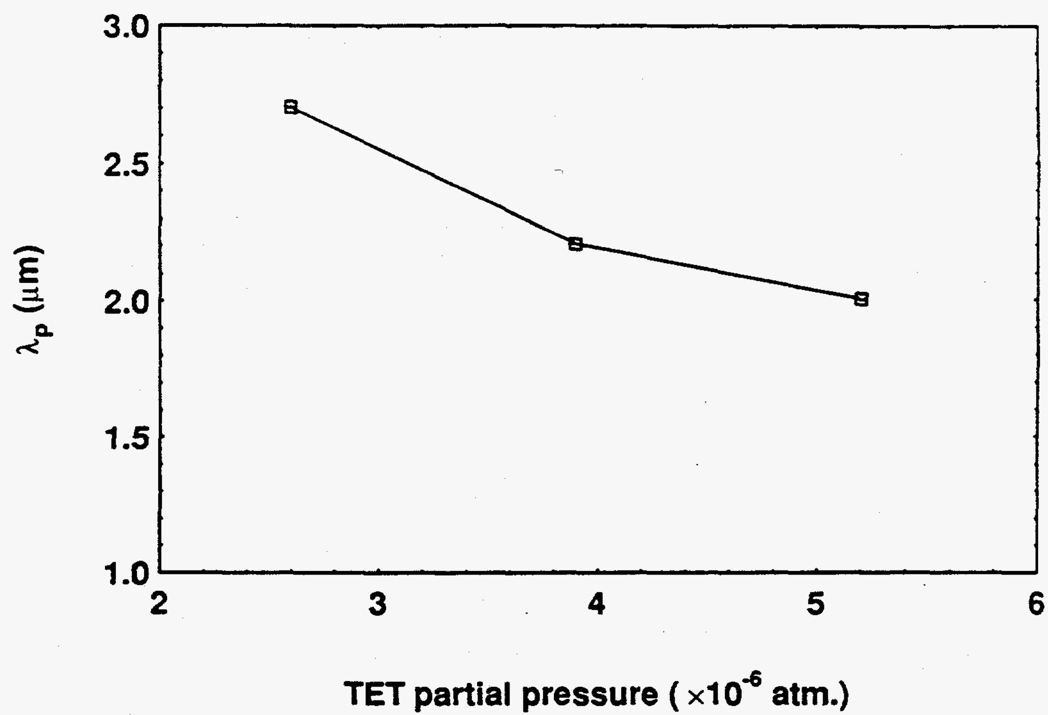

Fig.10 Variation of λ_p with TET partial pressure used during the growth of tin-doped In_2O_3. (Partial pressures of TMI and O_2 were kept constant at 1×10^{-4}atm and 3×10^{-3}atm respectively)

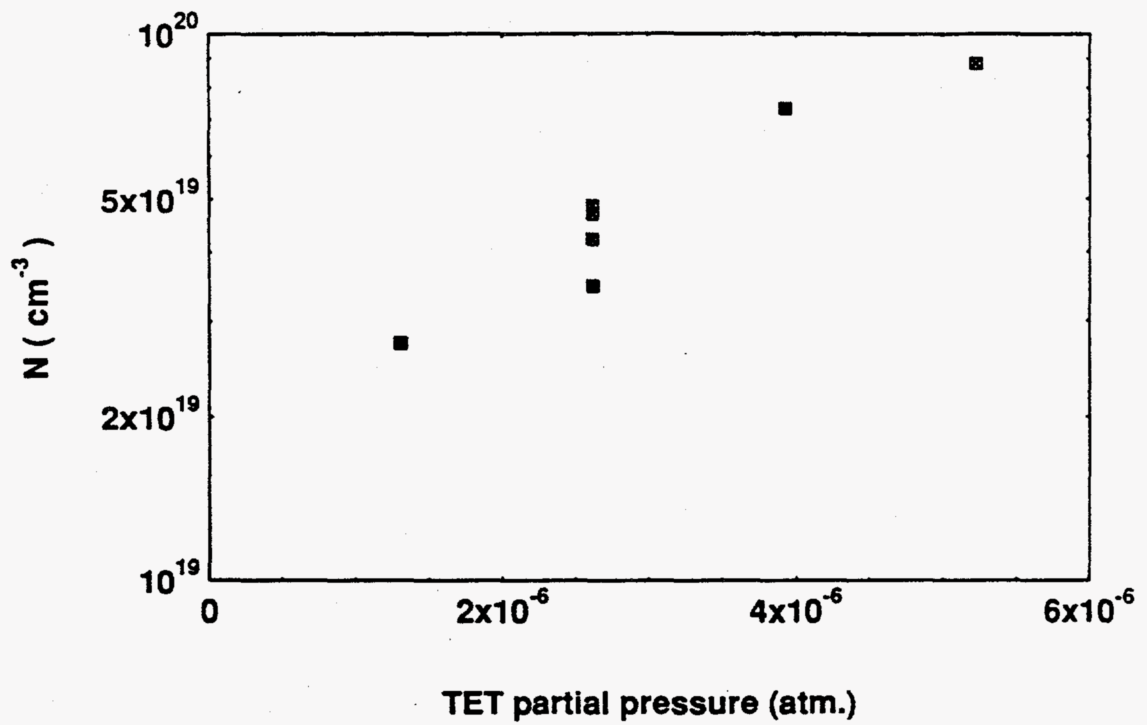

Fig. 11 Carrier concentration of tin-doped In_2O_3 layers vs. partial pressure of TET used during the growth.

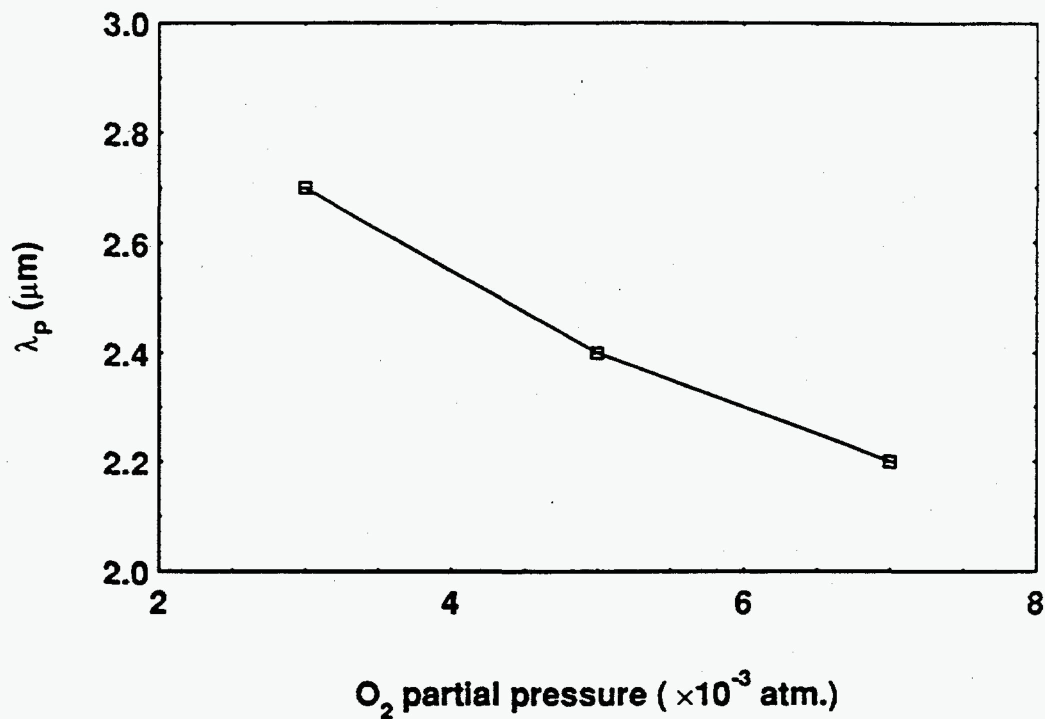

Fig. 12 Variation of λ_p with O_2 partial pressure used during the growth of tin-doped In_2O_3. (Partial pressures of TMI and TET were kept constant at 1×10^{-4}atm and 3.93×10^{-6}atm respectively).

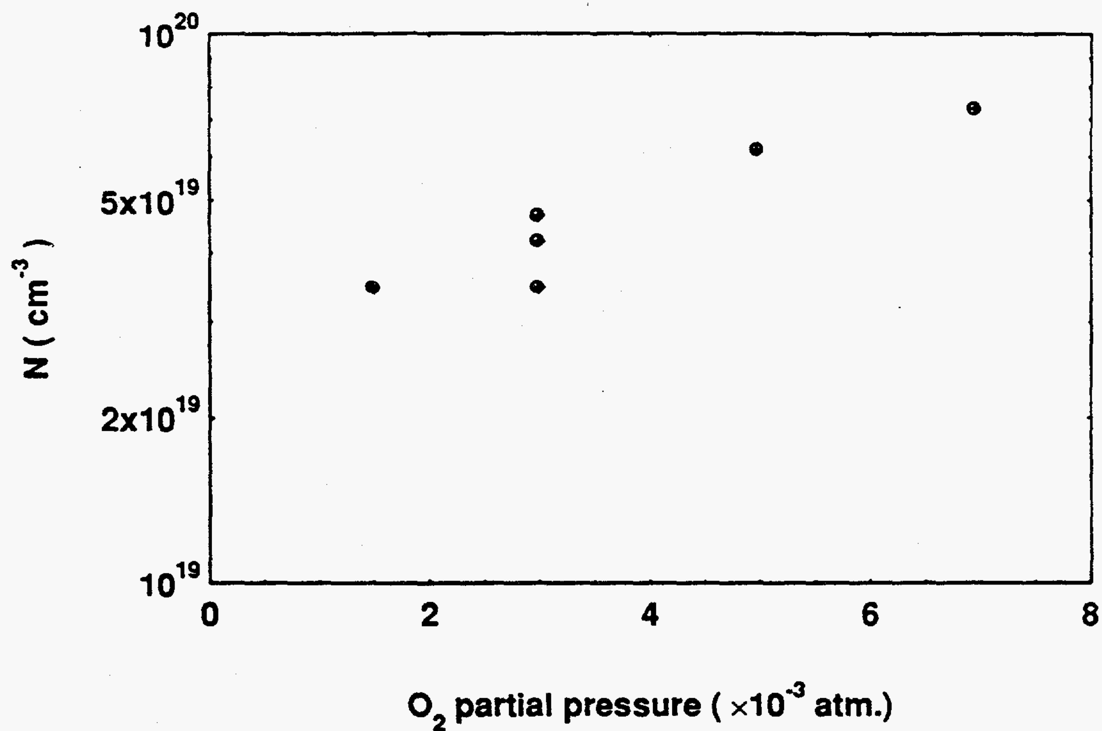

Fig. 13 Carrier concentration of tin-doped In_2O_3 layers vs. partial pressure of O_2 used during the growth.

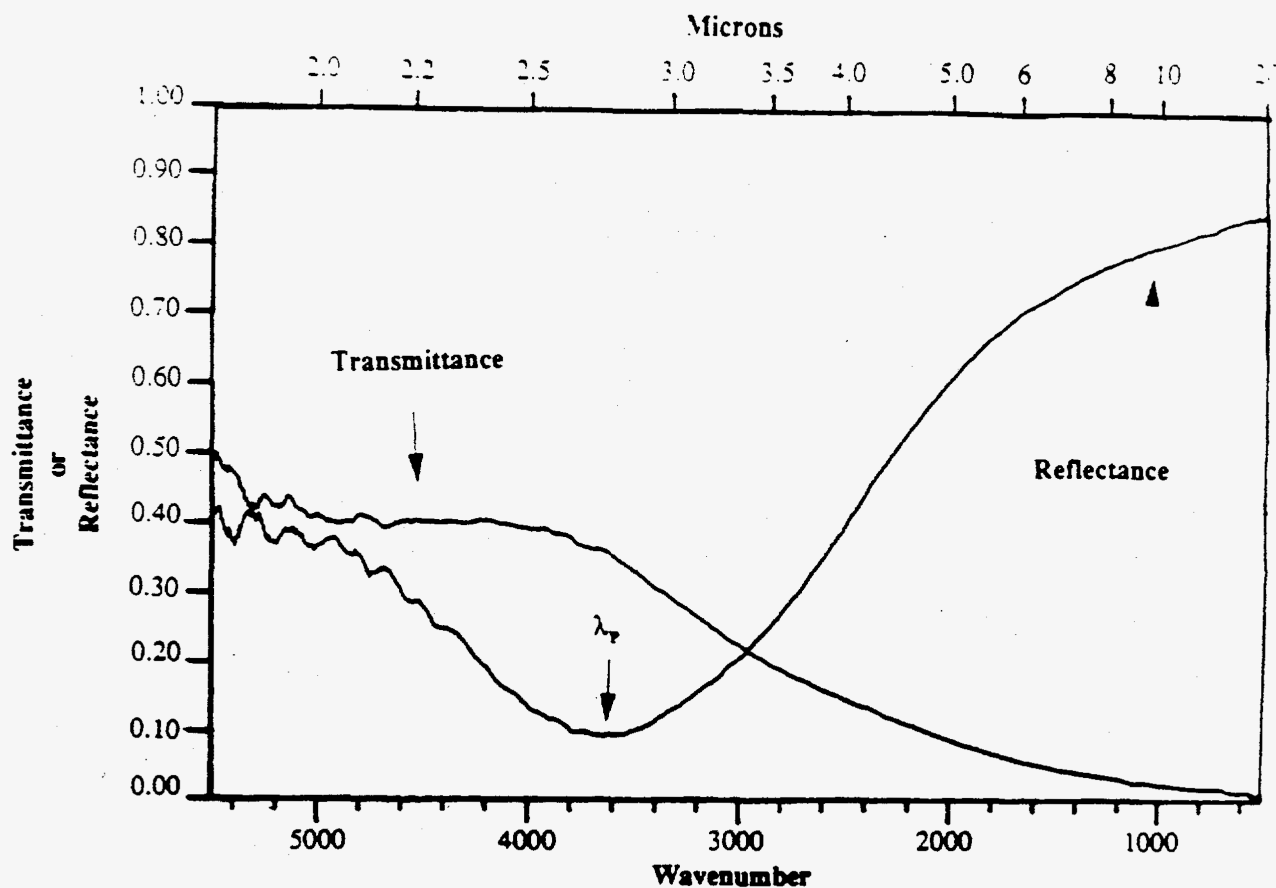

Fig. 14 Reflectance and transmittance spectra of tin-doped In_2O_3 grown on Si (100).

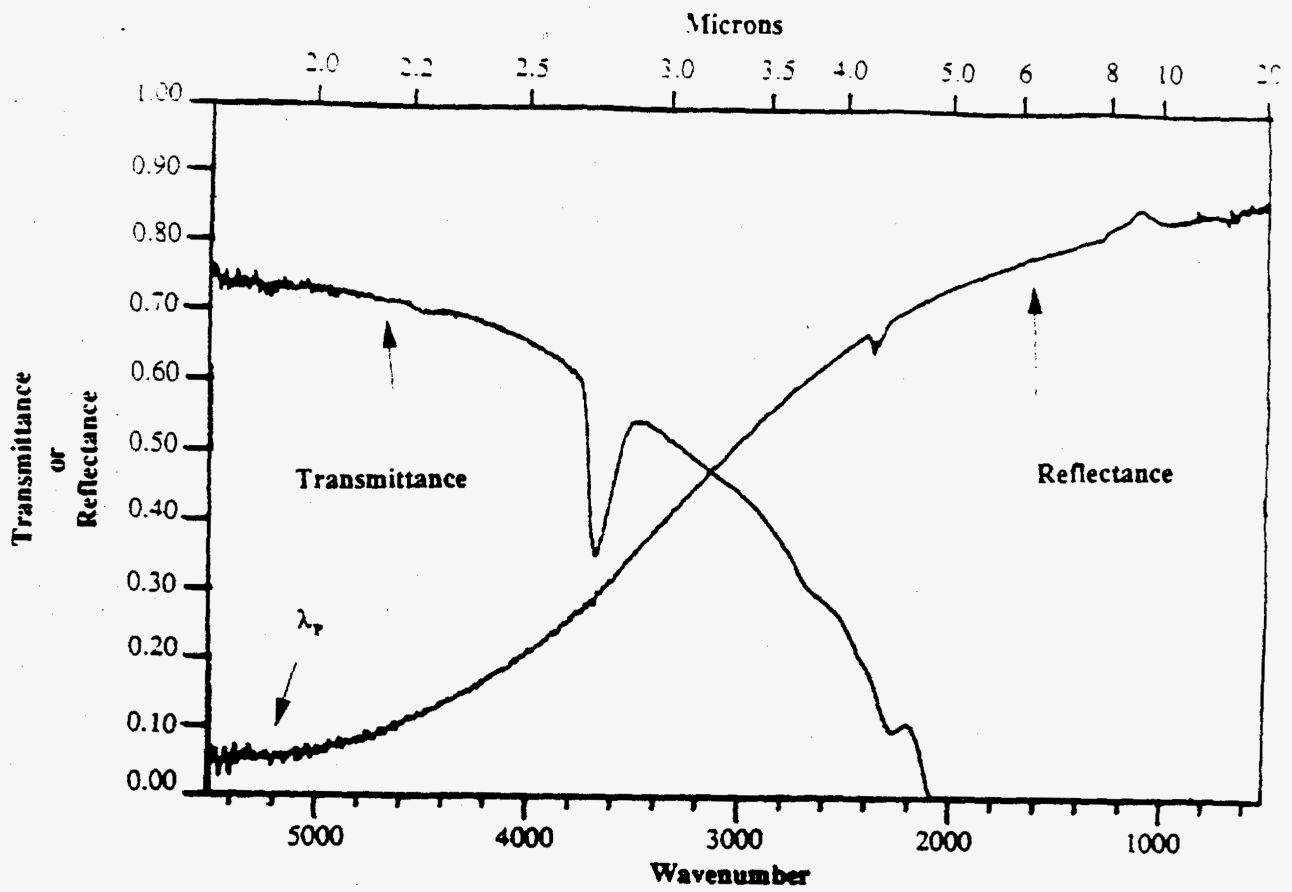

Fig. 15 Reflectance and transmittance spectra of tin-doped In_2O_3 grown on fused silica.

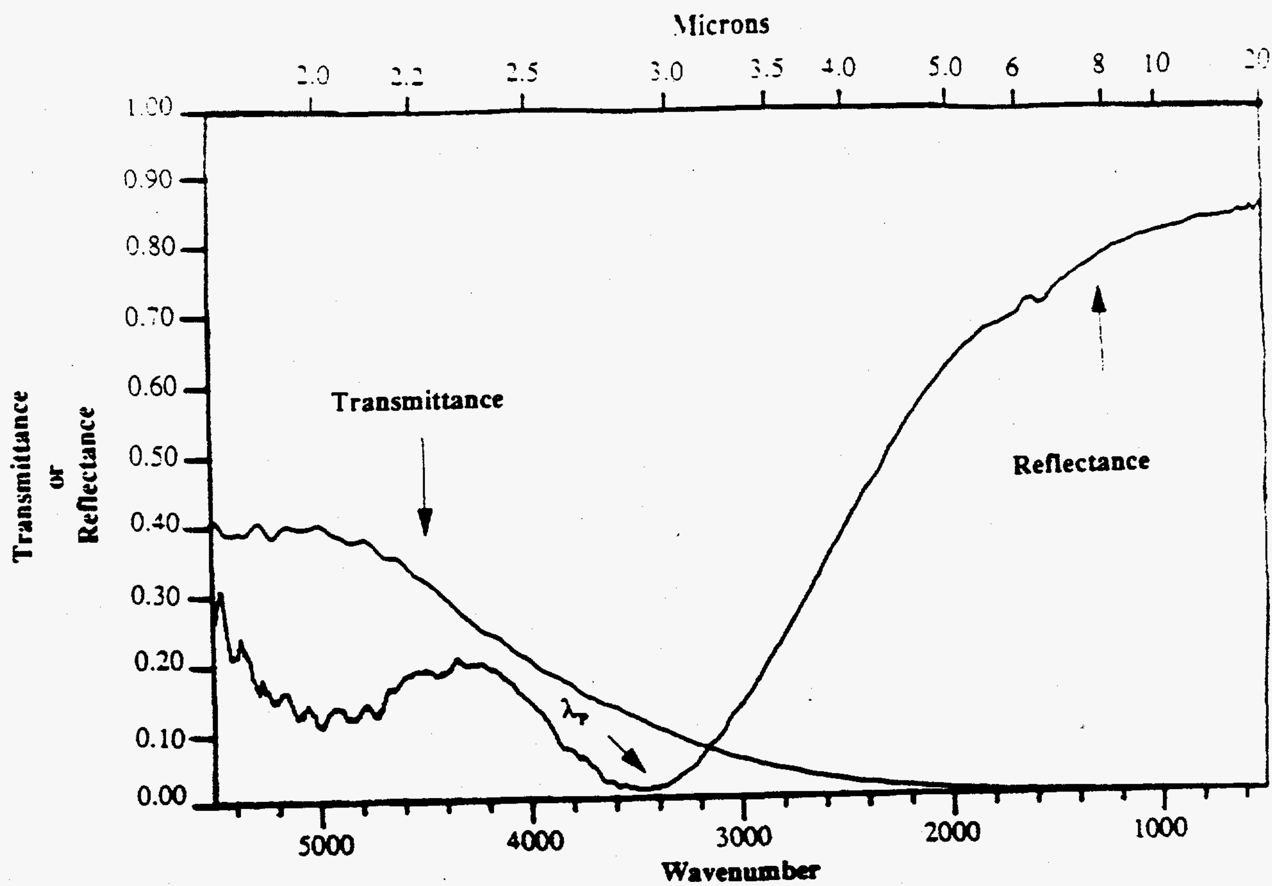

Fig. 16 Reflectance and transmittance spectra of tin-doped In_2O_3 grown on Si (100) to a thickness of 1.3μm (2 × normal thickness).

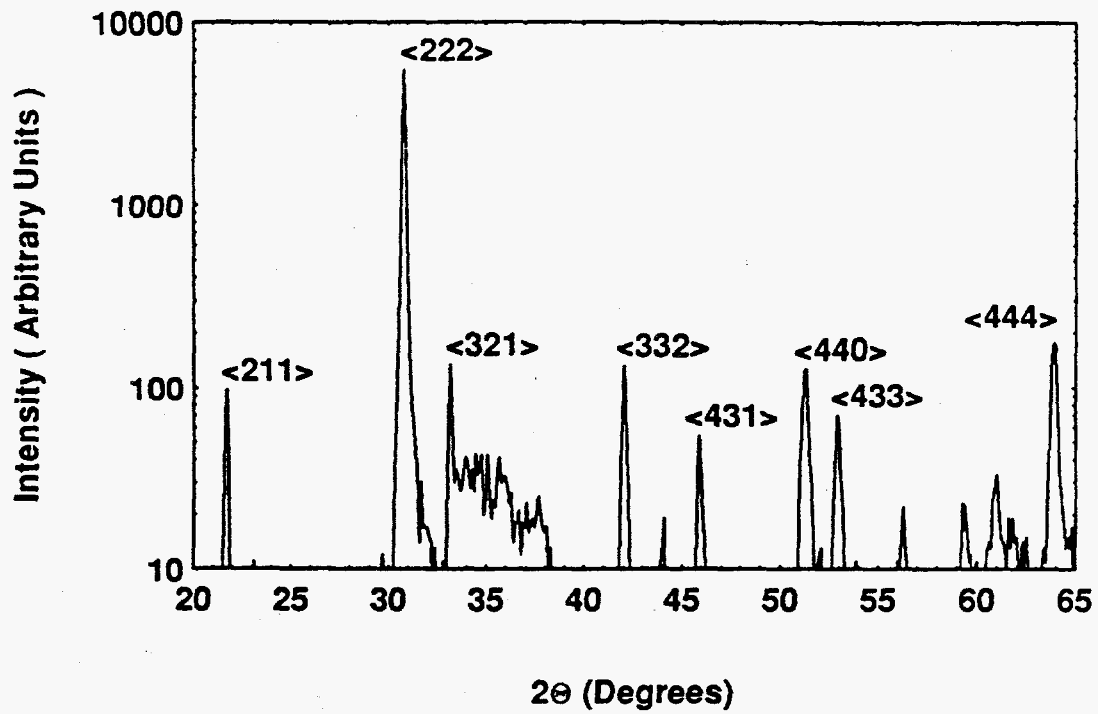

Fig. 17 Results of X-ray diffraction measurement on tin-doped In_2O_3 (Cu Kα radiation).